Chapter 3

Results

Contents

3.1 Bulk properties of ruthenium

Ruthenium is a platinium-group transition metal with a partly filled 5*s* and 4*d* shells in the free atom, usually designated as [Kr]$4d^7 5s^1$. The next state, 4*p*, is energetically already over 40 eV deeper in energy than the valence states and is thus very inert against taking actively part in chemical bonding in different chemical environments.[1] Under normal temperature and pressure conditions ruthenium crystallises in the hexagonal close-packed structure – *hcp* – shown in the Figure 3.1.

The electronic properties of bulk ruthenium can be described with the total density of states in the Figure 3.2, the electron orbitals projected on the atomic orbitals or the projected density of states in the Figure 3.3 and the band structure in the Figure 3.4. The bulk electronic structure can thus be simplified with the model presented in the Figure 3.6, consisting of an *s* band which starts

[1] However its absolute energetic position can change somewhat but this is not due to chemical hybridisation of orbitals but a core-level shift

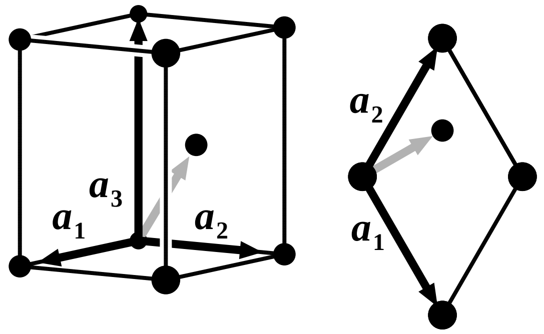

Figure 3.1: The hexagonal close packed structure. The basis vectors are $\mathbf{a}_1 = [1/2, -\sqrt{3}/2, 0]$, $\mathbf{a}_2 = [1/2, \sqrt{3}/2, 0]$ and $\mathbf{a}_3 = [0, 0, c/a]$ in the units of the lattice constant a; c/a is the other lattice parameter. The grey arrow shows the basis vector $[1/2, 1/(2\sqrt{3}), (c/a)/2]$

at deep energies and a rectangular *d* band which is cut off at the Fermi energy. The next clear feature after the *d* band in the total density of states does not begin until 12 eV above the Fermi energy. From the character table

D_{3h} ($\bar{6}2$)

			E	σ_h	$2C_3$	$2S_3$	$3C_2'$	$3\sigma_v$
$x^2+y^2,\ z^2$		A_1'	1	1	1	1	1	1
	R_z	A_2'	1	1	1	1	-1	-1
		A_1''	1	-1	1	-1	1	-1
	z	A_2''	1	-1	1	-1	-1	1
$(x^2-y^2,\ xy)$	(x,y)	E'	2	1	-1	-1	0	0
$(xz,\ yz)$	$(R_x,\ R_y)$	E''	2	-1	-1	1	0	0

of the D_{3h} symmetry group of the hexagonal close-packed crystal we see that the *p* orbitals p_x and p_y, and the *d* orbitals $d_{x^2-y^2}$ and d_{xy} are degenerate with each other, as are d_{xz} and d_{yz}. Therefore there are only three independent *d* orbitals, whereas *e.g.* in the bulk of a face centred crystal all the *d* orbitals are degenerate due to the higher symmetry than in the hexagonal close-packed crystal.

3.2 Clean Ru (0001) surface

The clean Ru (0001) consists of the close-packed hexagonal layers with a A-B-A-B stacking as seen in the Figure 3.7. The layer distance is simply $c/2$, and the atoms within the layers are located at the nearest-neighbour distance a.

The geometry of the clean surface was calculated several times with different number of atomic layers, number of layers allowed to relax and the exchange-correlation functional; the results are shown in the Figure 3.8. Except for the calculation with a plane wave cut-off of 68 Ry and 9 **k** points the converged values are $-3.0\ldots-3.3$ % within the generalised gradient approximation and -3.6 % within the local density approximation; we do not know the origin of the discrepancy. The clearly smaller relaxation obtained with only three **k** points is due to the badly converged sampling of the Brillouin zone. The deviation in the values by 0.3 % is not significant as this corresponds to about 5 mÅ and is thus much smaller than *e.g.* the discreteness of the mesh in the real space.

Experimentally the clean Ru (0001) is a benchmark before starting measurements with adsorbates, therefore during the years the relaxation of the surface has been repeatedly measured –

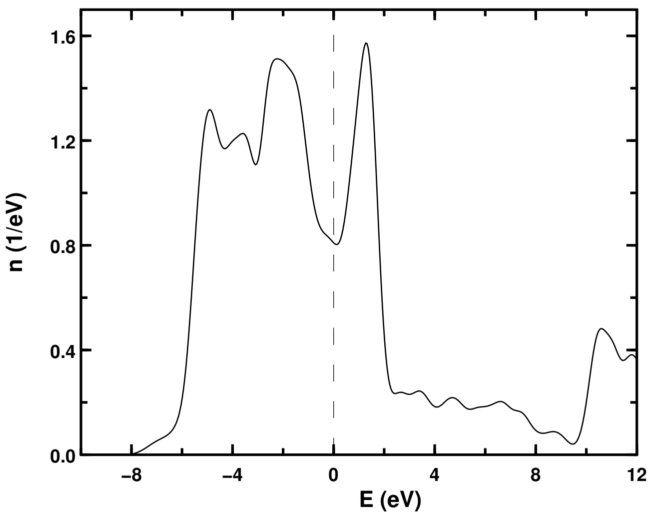

Figure 3.2: The density of states of bulk ruthenium calculated within the generalised gradient approximation of Perdew, Burke and Ernzerhof (1996). The Kohn-Sham eigenvalues were broadened with a Gaussian of decay parameter of 0.3 eV

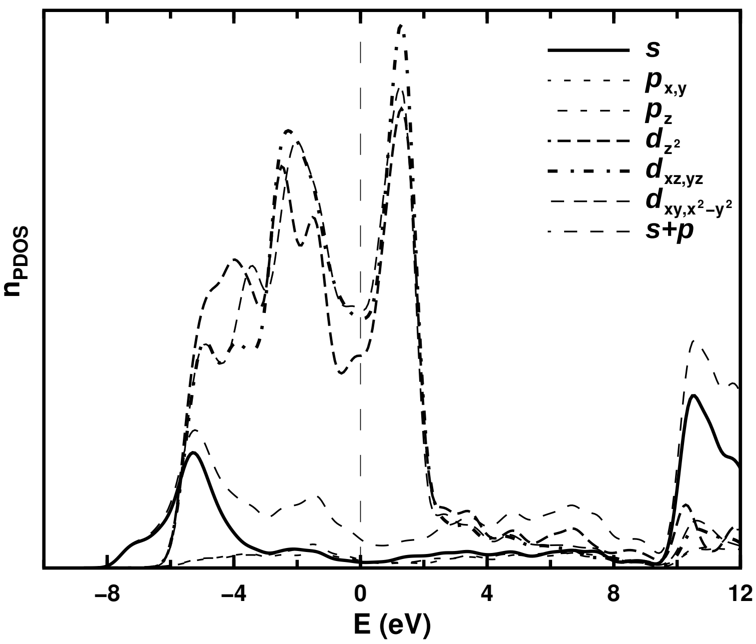

Figure 3.3: The projected density of states of bulk ruthenium calculated within the generalised gradient approximation of Perdew, Burke and Ernzerhof (1996). The Kohn-Sham eigenvalues were broadened with a Gaussian of decay parameter of 0.3 eV

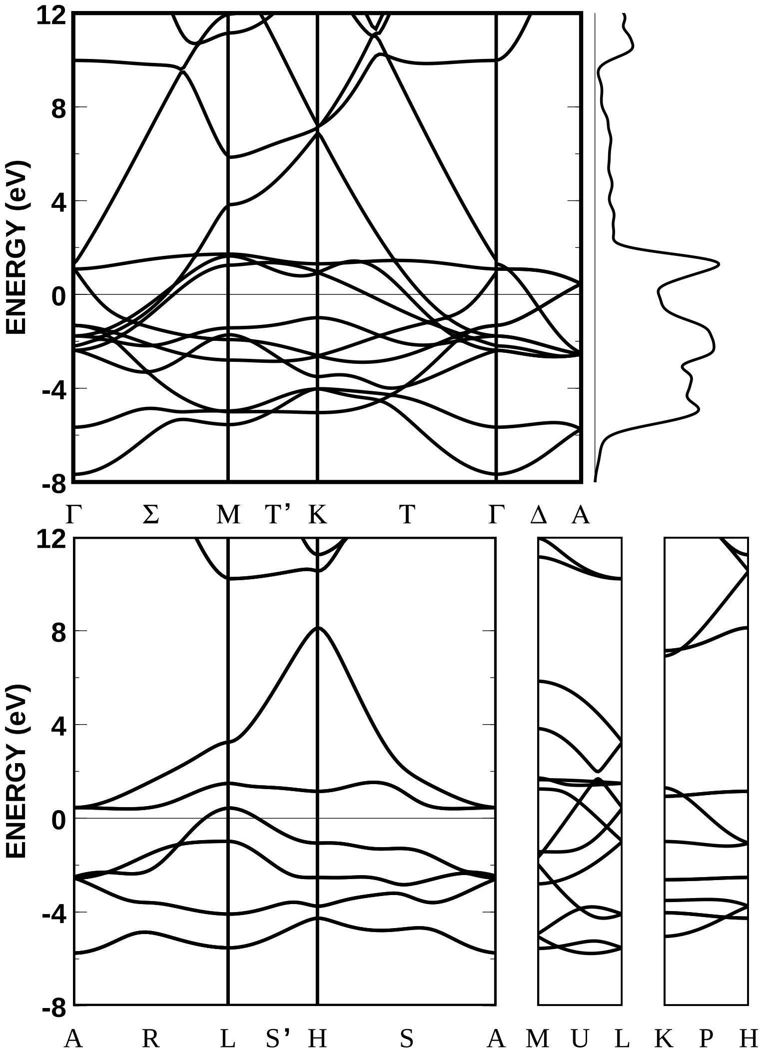

Figure 3.4: The band structure of bulk ruthenium calculated from the Kohn-Sham eigenvalues within the generalised gradient approximation of Perdew, Burke and Ernzerhof (1996). The Brillouin zone of the crystal and the labelling of the **k** points and high-symmetry lines are shown in the Figure 3.5

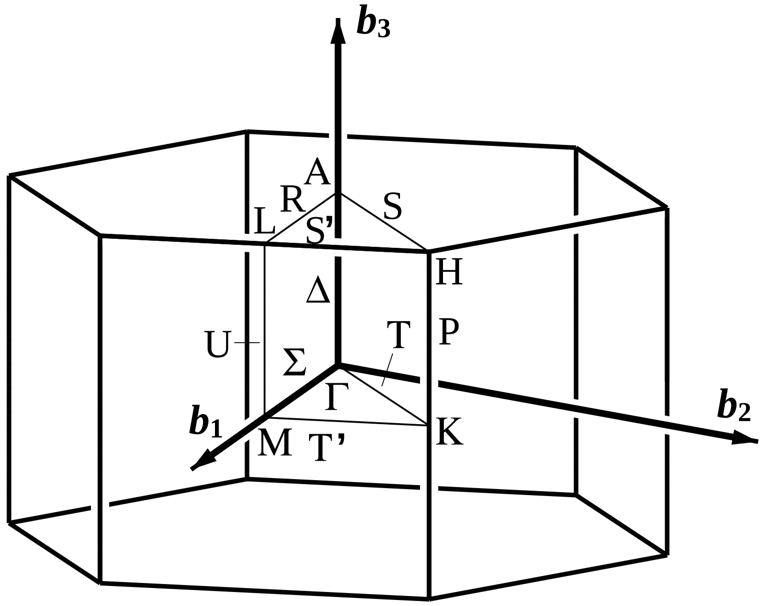

Figure 3.5: The Brillouin zone and the labelling of the **k** points and high-symmetry lines of the hexagonal close-packed structure

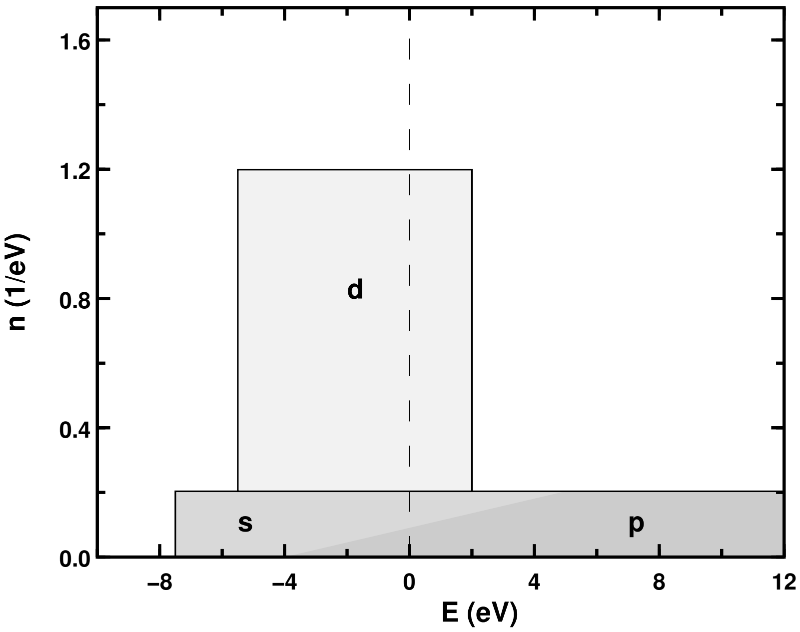

Figure 3.6: A model for the density of states of bulk ruthenium

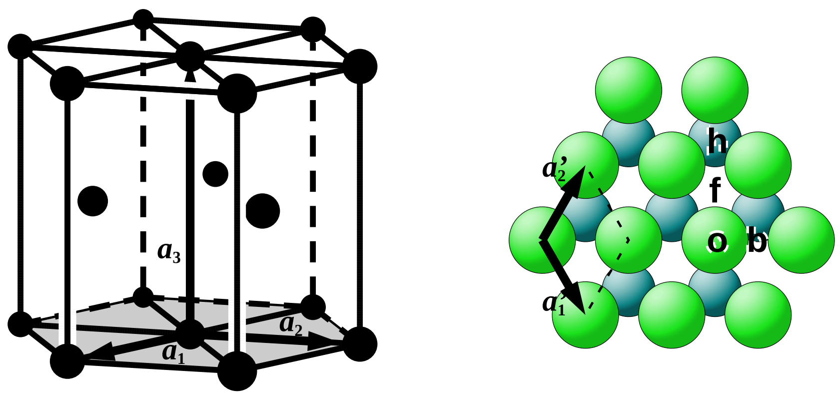

Figure 3.7: The cut of the (0001) surface from the hcp crystal; the stacking is A-B-A-B, and the high-coordinated adsorption sites have been indicated with *o*, *h*, *f* and *b* for on-top, hcp, fcc and bridge sites, respectively

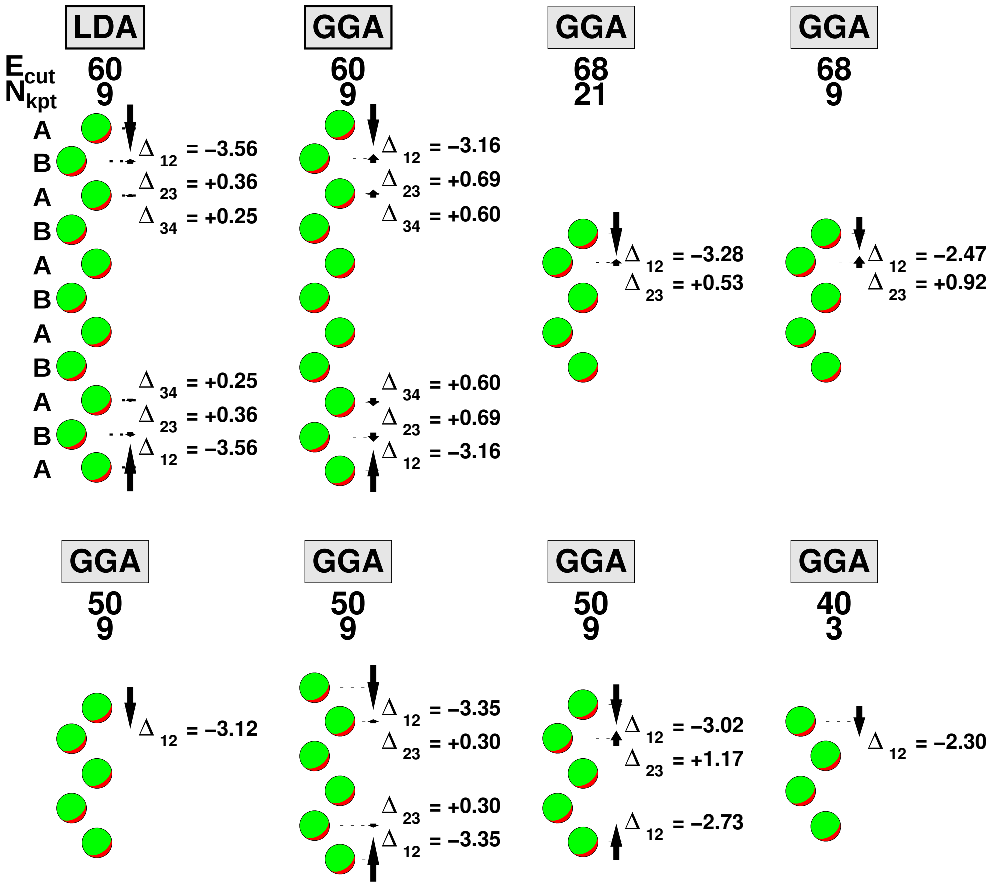

Figure 3.8: The relaxation of the clean (0001) surface obtained with different calculational parameters and exchange-correlation functionals; the values are in per cent of the corresponding distance in the ideal bulk structure

please see Menzel (1997). The outer-most layer distance 2.09±0.015 Å at temperatures between 120 and 300 K corresponds to a contraction of $\Delta_{12} = -2.3 \pm 0.7$ % and between 20 and 50 K to $\Delta_{12} = -2.8$ %, and thus the theoretical values are not too far from the experiments. An attempt (Feibelman *et al*, 1994) to explain the systematic overestimation of the absolute value of the magnitude of the outer-most layer expansion by hydrogen contamination was promptly rejected (Menzel, 1994). The contraction of the outer-most layer relaxation is a general trend among the transition metals (Methfessel, Hennig & Scheffler, 1992) and is due to the removed nearest-neighbour atoms of the first layer, causing the outer-most layer to relax towards the second layer in order to strengthen the bonding between the atoms at the first and second layer.

The surface band structure at Ru (0001) is shown in the Figure 3.9; gaps in the projected bulk band structure appear at all energies from five electron volts below to well above the Fermi energy, and the most notable ones below the Fermi energy are at $\bar{\Gamma}$ around -4 eV and at -2 eV at $\bar{K}$, and at the Fermi energy at the line between $\bar{\Gamma}$ and $\bar{K}$. The surface states found in these gaps are shown in the Figure 3.10. In the gap above the Fermi energy there appear some states at energies expected for the image states; however, by inspection of the density profile of these states along the surface normal in the Figure 3.11 it is obvious that even if they would be related to the real image states the vacuum region is too small for the states to decay; furthermore, the generalised gradient approximation should not lead to the formation of image states because its asymptotic form does not approach the $\propto \frac{1}{z}$ which creates the image potential. Thereby the states in the band gaps, *e.g.* between 4 and 10 eV above the Fermi energy at the $\bar{\Gamma}$, are an artifact of the slab geometry, leading to an effective potential well for these states; the lower potential in the vacuum than inside the slab for these electrons is due to the ortho-normalisation of these states against the states in the slab, making the slab region effectively more repulsive to these states. Furthermore at the Fermi energy there should be a continuum of states but these are forced into the series of states with increasing number of nodes and thus energy due to the localisation to the region between the slabs.

We also calculated the iso-electronic reactivity function of Wilke *et al* for the surface – please see Section 2.5.7; the result is shown in the Figure 3.12. The first qualitative observation is that the magnitude of $\mathcal{W}_{\mathrm{N}}$ is largest at the d orbitals around the surface atoms: the d_{z^2} and d_{xy,x^2-y^2} orbitals are occupied but easily emptied – blue regions – and the $d_{xz,yz}$ are unoccupied but easily occupied – red regions. A second, more de-localised, effect is the distribution of the reactivity function above the three-fold hollow and on-top adsorption places. This is somewhat complicated because the reactivity function changes its sign when approaching the surface. However at the typical bonding height of $2p$ elements on Ru (0001) – about 1.2 Å – the initially unoccupied $d_{xz,yz}$ orbitals point out towards the hcp site and interestingly much less towards the fcc site; at the on-top site a large number of d_{z^2} provide easily emptied orbitals. Thus a typical situation occurring when adsorbing an electronegative element could be that the $d_{xz,yz}$ orbitals become occupied, leading to a better screening and bonding with the adsorbate while the d_{z^2} orbitals are emptied. An adsorbate more electropositive than this surface would most easily donate some charge density to the surface to the $d_{xz,yz}$ orbitals. However, it is very important to notice that the reactivity function simulates only tiny changes around the Fermi energy whereas chemisorption leads to chemical bonds often several electron volts away from the Fermi energy.

It is instructive to compare the reactivity function with the projected density of density, given in the Figure 3.13: the main change in the projected density of density at the surface relative to bulk is the narrowing of the d band due to the reduced coordination of the surface atoms. Around the

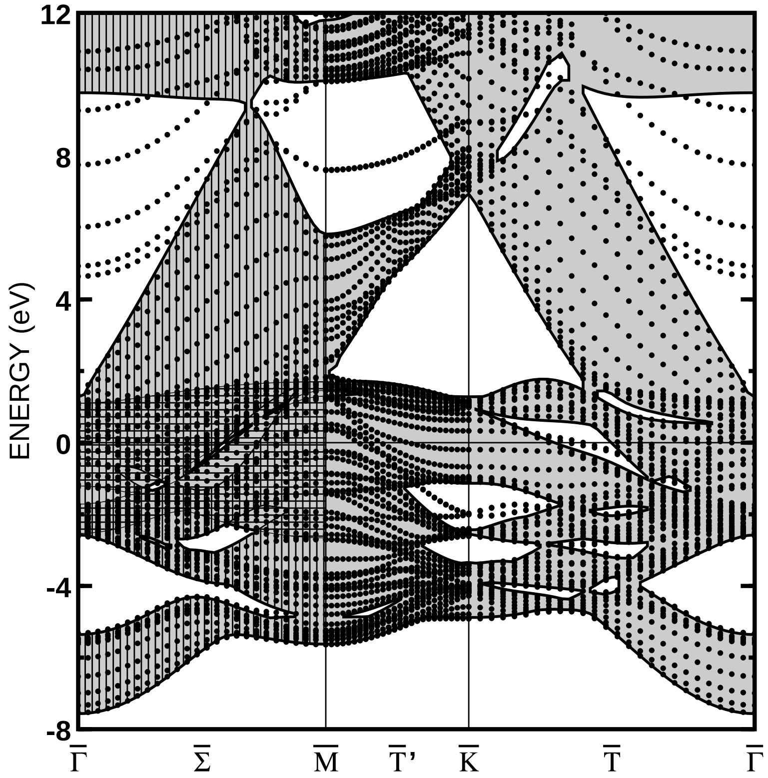

Figure 3.9: The band structure of the clean (0001) surface of ruthenium; the projected band structure of the bulk is shown with the gray areas, and the vertically and horisontally hatched regions between the points $\bar{\Gamma}$ and $\bar{M}$ correspond to states with even and odd symmetry with respect to the mirror plane

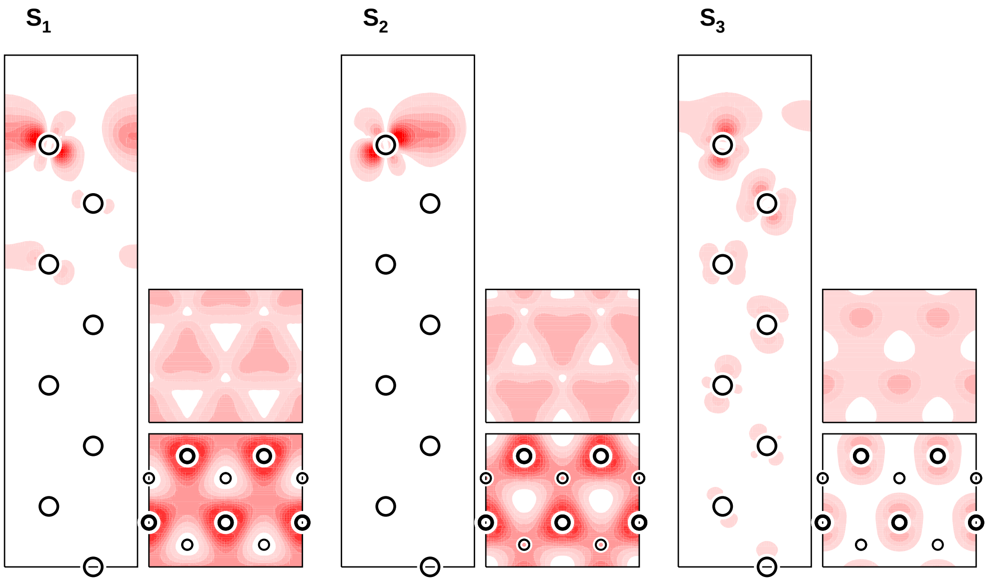

Figure 3.10: The surface states – obtained from the Kohn-Sham orbitals – at the clean (0001) surface of ruthenium at **k** points $\bar{K}$ – S_1 and S_2 – and $\bar{T} \approx 2/3\,(\bar{\Gamma} \rightarrow \bar{K})$ – S_3. The cuts along the surface are taken at the surface plane and 1 Å above it, and the cut in the plane through half of the slab is vertical at the centre of the lateral cuts

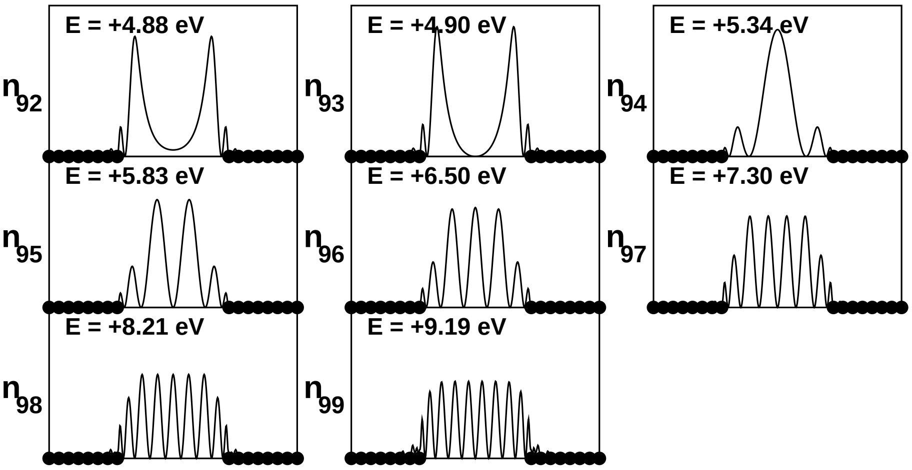

Figure 3.11: The density profiles of Kohn-Sham states at Ru (0001) at the $\bar{\Gamma}$ point in the Brillouin zone; the states are located in the vacuum region – the atomic positions are denoted with filled spheres and are caused by the image potential and repulsion from the states in the slab. The Kohn-Sham eigenvalues are normalised to the Fermi energy and the vacuum level of the potential is at the work function of the surface *i. e.* 5.0 eV

Fermi energy the d_{z^2} narrows most, bringing the peak in the projected band structure to intersect the Fermi energy; the reactivity function suggests that these orbitals are then easily pushed up in the energy and thus emptied. The other d orbitals have rather a constant magnitude near the Fermi energy and thus the effects in the reactivity functions are due to some redistribution of these orbitals. It is also easy to understand the small amplitude of the reactivity function in the bulk layers by inspection of the amount of d orbitals in the vicinity of the Fermi energy in the Figure 3.13: all the different bands have almost a constant amplitude, thus leading to small changes when changes occur.

Please notice that the degeneracy of the d orbitals prevails from the bulk because the crystal is cut parallel to the high-symmetry axis of the hexagonal close-packed surface; the mirror planes parallel and rotations with the axis along the surface are removed, though. The symmetry group is C_{3v} whose character table is as follows:

C_{3v} $(3m)$

			E	$2C_3$	$3\sigma_v$
$x^2+y^2,\ z^2$	z	A_1	1	1	1
	R_z	A_2	1	1	-1
$(x^2-y^2,\ xy)$ $(xz,\ yz)$	(x,y) $(R_x,\ R_y)$	E	2	-1	0

Thus the same degeneracies – p_x and p_y, $d_{x^2-y^2}$ and d_{xy}, d_{xz} and d_{yz} – prevail; this is expected since all the orbital pairs are identical by a rotation along the three-fold axis, which remains intact at the surface, this rotational identity remains despite the lowering of the overall symmetry. On all the other surfaces this will no longer hold and thus degeneracies will be lost.

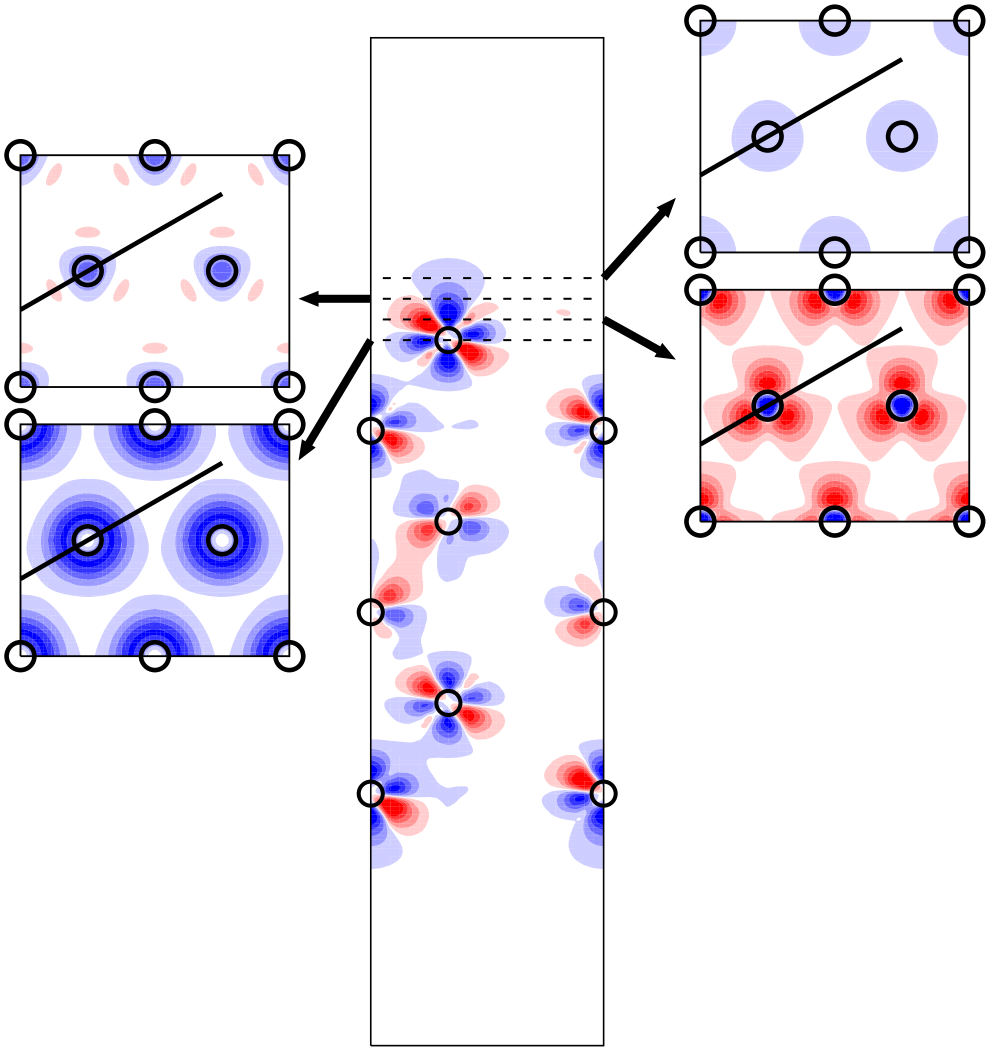

Figure 3.12: The reactivity function of Wilke, Cohen and Scheffler for the clean (0001) surface of ruthenium. The positive – red – regions correlate with unoccupied and the negative – blue – regions with occupied orbitals, the former becoming easily occupied and the latter easily emptied. The black line in the small cuts along the surface show the position of the vertical cut

Table 3.1: The centre and the width – calculated from the standard deviation – of the d band from the projected density of states

layer	d_{z^2}	$d_{xz,yz}$	$d_{x^2-y^2,xy}$	d_{total}
Surface	-1.3 / 4.0	-1.0 / 4.0	-1.1 / 4.4	-1.1 / 4.2
Sub-surface	-1.6 / 5.1	-1.4 / 4.7	-1.5 / 4.7	-1.5 / 4.8
Middle (bulk)	-1.5 / 4.9	-1.3 / 4.6	-1.3 / 4.6	-1.3 / 4.7

Table 3.2: The integral of the projected density of states multiplied with the occupation numbers

layer	s	$p_{x,y}$	p_z	d_{z^2}	$d_{xz,yz}$	$d_{x^2-y^2,xy}$
Surface	0.26	0.06	0.04	1.08	1.10	1.08
Sub-surface	0.26	0.07	0.08	1.12	1.05	1.11
Middle (bulk)	0.26	0.07	0.08	1.08	1.09	1.10

layer	s	p	d
Surface	0.26	0.16	5.44
Sub-surface	0.26	0.22	5.44
Middle (bulk)	0.26	0.21	5.44

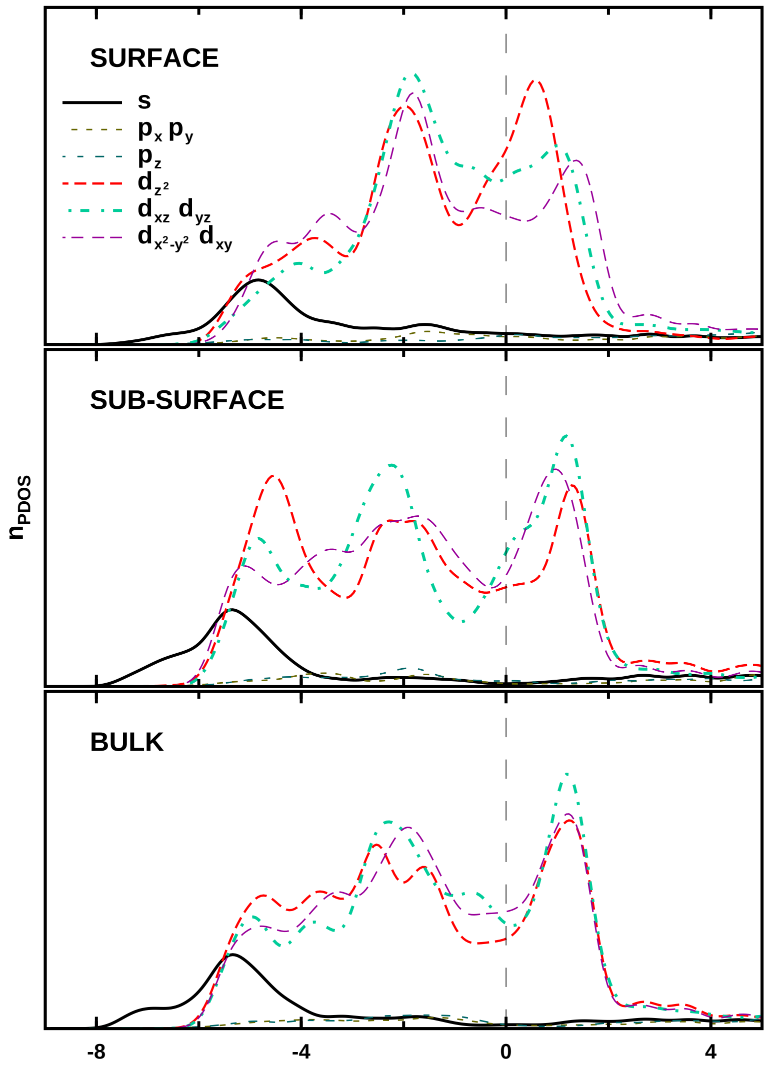

Figure 3.13: The projected density of states of the (0001) surface of ruthenium